HHS Public Access

Author manuscript

Arterioscler Thromb Vasc Biol. Author manuscript; available in PMC 2024 July 01.

Published in final edited form as:

Arterioscler Thromb Vasc Biol. 2023 July ; 43(7): e231–e237. doi:10.1161/ATVBAHA.122.318622.

Mesenchymal stromal cells facilitate tip cell fusion downstream of BMP-mediated venous angiogenesis

Shahram Eisa-Beygi[1], **Meng-Ming Hu**[1], **Suresh N Kumar**[2], **Brooke E Jeffery**[1], **Ross F Collery**[1,3], **Nghia Jack Vo**[4,5], **Bhawika S Lamichanne**[6], **H Joseph Yost**[6], **Matthew B Veldman**[1], **Brian A Link**[1]

[1]Department of Cell Biology, Neurobiology and Anatomy, Medical College of Wisconsin, Milwaukee

[2]Department of Pathology, Medical College of Wisconsin, Milwaukee

[3]Department of Ophthalmology and Visual Sciences, Medical College of Wisconsin, Milwaukee

[4]Department of Radiology, Medical College of Wisconsin, Milwaukee

[5]Department of Radiology, Pediatric Imaging and Interventional Radiology, Children's Hospital of Wisconsin, Milwaukee

[6]Molecular Medicine Program, Eccles Institute of Human Genetics, University of Utah, Salt Lake City

Abstract

Background: The goal of this study was to identify and characterize cell-cell interactions that facilitate endothelial tip cell fusion downstream of Bone Morphogenic Protein (BMP)-mediated venous plexus formation.

Methods: High resolution and time-lapse imaging of transgenic reporter lines and loss-of-function studies were carried out to study the involvement of mesenchymal stromal cells (SCs) during venous angiogenesis.

Results: BMP-responsive SCs facilitate timely and precise fusion of venous tip cells during developmental angiogenesis.

Conclusion: SCs are required for anastomosis of venous tip cells in the embryonic caudal hematopoietic tissue (CHT).

Graphical Abstract

Disclosures: None

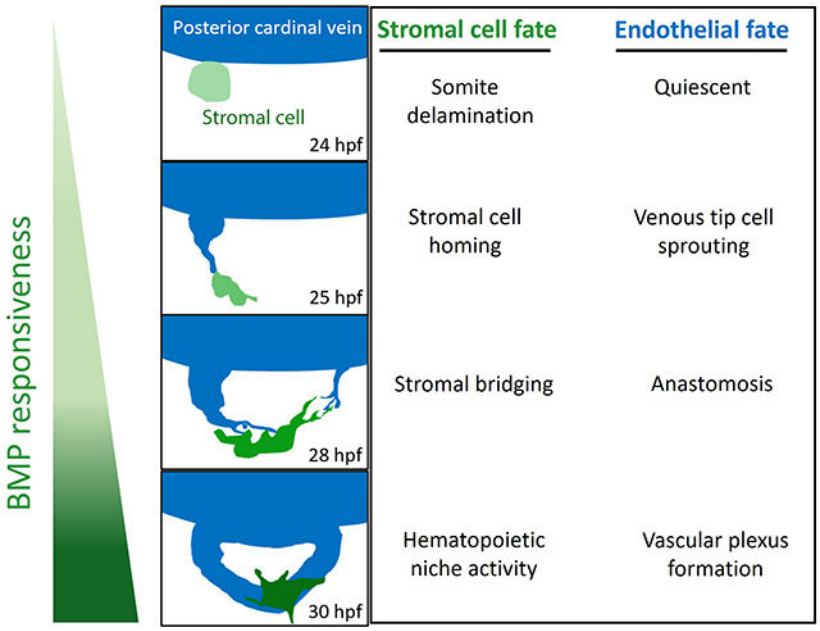

Keywords

Mesenchymal Stromal Cells; BMP signaling; anastomosis; angiogenesis; arteriovenous development; zebrafish

Introduction:

Establishment of tissue-specific vessel networks often involves transient crosstalk between endothelial cells (ECs) and their immediate micro-environment that regulate the direction and extent of angiogenesis.[1–6] In addition to enacting control over tip cell sprouting and migration, microenvironmental cues facilitate fusion of adjacent tip cells, a process known as *anastomosis*.[7] Sites of anastomosis are frequently occupied by tissue resident macrophages that act as scaffolds or chaperones, enabling tip cells to slide along their surfaces and fuse together.[2,8] These endothelial-macrophage interactions occur downstream of tip cell induction and sprouting events guided by the vascular endothelial growth factor (VEGF-A) in both fish and mammalian models of vascularization.[2,8] VEGF-A is a stimulant of arterial specification.[2,8,9]. In contrast, venous specification and angiogenesis are primarily mediated by bone morphogenetic protein (BMP) signaling in fish, mammals and birds.[9,10,11] However, it is unknown whether venous tip cell anastomosis relies on chaperone cells to ensure proper tip cell fusion.

To study tip cell anastomosis downstream of BMP signaling, we focused on the caudal vein plexus (CVP), the densely vascularized hematopoietic niche in embryonic zebrafish, analogous to the fetal liver in mammals, which forms via Bmp signaling.[9] At 24 hpf, the zebrafish embryo has developed two axial vessels positioned along its medial side, namely, the dorsal artery (DA) and posterior cardinal vein (PCV) (Figure 1A, upper panel). The arterial-fated intersomitic vessels (ISVs) arise from the DA and migrate dorsally along

somite boundaries, responding to somite-derived Vegfa gradients. At approximately the same time, venous sprouts emanate from the PCV and migrate ventrally in response to Bmp2 gradients and form multiple sites of anastomosis (Figure 1A, upper panel). Through a sequence of sprouting, fusion, and reorganization of these Bmp-responsive tip cells at the angiogenic front, a honeycomb-like vascular plexus is formed by 48 hpf, which also serves as the caudal hematopoietic tissue (CHT) in the embryo. However, the mechanisms mediating the anastomosis of these venous tip cells remain unknown.

Materials and Methods:

The authors declare that all supporting data are available within the article (and in the online-only Data Supplement).

Zebrafish Husbandry, Transgenic and Mutant lines:

The following zebrafish lines were used in this study: ZDR genetic background (wild-type) fish (originally purchased from Aquatica Biotech, Sun City Center, Florida), *Tg(fli1:EGFP)*^{y1}, *Tg(6.5kdrl:mCherry)*^{ci5}, *Tg(BRE:eGFP)*, *Tg(BRE:d2GFP)*, *Tg(mpeg1:GFP)*, *Tg(TCF-nls:mCherry)* and the recessive maternal zygotic (MZ) syndecan 2 (*sdc2−/−*) line.[12] Adult zebrafish were housed at a water temperature of ~28.0°C and were subjected to a 14-hour light: 10-hour dark photoperiod at the Medical College of Wisconsin Fish Facility. All animal experiments were approved by the Institutional Animal Care and Use Committee of the Medical College of Wisconsin. Freshly fertilized embryos were procured through natural breeding of adult zebrafish and were kept at ~28.0°C in 1X E3 embryo medium (E3 medium) containing 5 mmol/L NaCl, 0.17 mmol/L KCl, 0.33 mmol/L CaCl2, 0.33 mmol/L MgSO4, and 0.05% methylene blue. In some instances, embryos were treated with 0.003% of 1-phenyl-2-thiourea (Sigma-Aldrich), starting at 24 hours post fertilization (hpf), to minimize pigmentation.

Confocal microscopy and Laser Ablation of Stromal Cells:

For confocal microscopy analysis, embryos, at various developmental stages, were embedded in 1.5% low melting agarose in E3 medium and 30 μg/mL tricaine mesylate (ethyl 3-aminobenzoate methanesulfonate; Sigma-Aldrich) to induce mild anesthesia and immobilization. Embryos were mounted on 35 mm glass-bottom Petri dishes (CELLVIS). Multiple Z-stacks were acquired using a Zeiss LSM 510 AxioImager 2-photon & confocal microscope. All fluorescent image data were collected using a Carl Zeiss LSM 510 laser scanning microscope (Jena, Germany) equipped with a plan-apochromat ×20/0.8 numerical aperture (NA) lens and a C-apochromat ×40/1.1 NA lens. Images were collected (pinhole set at 1 airy unit) with appropriate dichroics and filters for each fluorescent protein. Image pixel saturation was corrected with photomultiplier tube detector gain and offset controls, as per the manufacturers' instructions. Projections of summed Z-stacks and enhancement of brightness and contrast were adjusted using the ImageJ/Fiji software (National Institutes of Health). For laser ablation of SCs, we used infrared 800 nm laser to irradiate all SCs (ranging from 1 to 4) that were in close apposition to putative sites of anastomosis, according to a previously established laser-based ablation protocol, with modifications to the laser wavelength, power and scan time.[13]

Wholemount Immunofluorescence:

Embryos were fixed in 4% paraformaldehyde (PFA)/1X Phosphate Buffered Saline Tween-20 (PBST) overnight at 4°C. After dehydration in 100% methanol and rehydration, embryos were permeabilized in ice-cold Acetone, blocked in 5% goat serum and incubated in rabbit mAb antibody against P-Smad1/5/8 (D5B10, Cell Signaling Technology) overnight at 4°C with gentle shaking. Following washes in 1X PBST, embryos were incubated for 1 hour in secondary antibody (Alexafluor 594nm, goat-anti rabbit, Catalog# A-11012, Thermo Fisher Scientific) at RT and imaged after several washes in 1X PBST.

Morpholino oligonucleotides:

To stop cardiac contractions and inhibit CVP formation, we used a morpholino oligonucleotide (MO) targeting the ATG translation-start site of cardiac troponin T type 2a, *tnnt2a* (MO:*tnnt2a*^{ATG}). As a negative control, we used a standard control MO (control MO) specific to a human β-globin intron mutation. All MOs were synthesized by GeneTools (Oregon). The MO sequences were:

MO:*tnnt2a*^{ATG}: 5'-CATGTTTGCTCTGATCTGACACGCA-3'

Control MO: 5'-CCTCTTACCTCAGTTACAATTTATA-3'

Prior to injection, MO solutions were briefly heated at 65°C and resuspended in 1X Danieau's solution (58 mmol/L NaCl, 0.7 mmol/L KCl, 0.4 mmol/L $MgSO_4$, 0.6 mmol/L $Ca(NO_3)_2$, 5.0 mmol/L HEPES, pH 7.6), and 0.1% (w/v) phenol red dye (Sigma-Aldrich), to a final concentration of 8 ng/nL. Embryos at 1-16 cell-stages were positioned in individual grooves made on a 1.5% agarose gel and injected with MOs at concentrations ranging from 0.5 to 6 ng/nL.

Statistical Analysis:

All data have been analyzed for normality and equal variance as a pre-condition before statistical analysis and for all statistical analysis, an unpaired students' t-test was used to compare the means of two groups. P values <0.05 were considered to indicate significant differences.

Results and Discussion:

Based on studies in zebrafish and mice, endothelial tip cell anastomosis downstream of VEGF signaling is mediated by macrophages acting as "bridge cells".[2,8] We sought to determine if macrophages played a similar inductive function in facilitating venous tip cell fusion downstream of BMP signaling. To test whether macrophages act as universal chaperone cells for tip cell anastomosis, we used the *Tg(mpeg1:GFP);(kdrl:mCherry)* line to simultaneously visualize macrophages and venous tip cells during development of CVP. Confocal analysis of the emerging CVP between 26 hpf and 28 hpf revealed a scarce population of mpeg1+ macrophages in this region where only 2.4% of all putative sites of anastomosis were occupied by macrophages (N: 8 fish imaged) (Figure I in the online-only Data Supplement). However, differential phase contrast microscopy revealed that almost all sites between neighboring venous tip cells were interposed by mesenchymal-shaped cells

that were neither of macrophage nor of endothelial lineage (Figure IIA–C in the online-only Data Supplement). Next, given that Bmp guidance is required for the formation of CVP,[9] we resorted to a Bmp activity reporter line previously generated in our lab to determine if these mesenchymal-shaped cells were Bmp-responsive.[14] In the *Tg(BRE:eGFP)* line, the Bmp-response element (BRE) derived from mouse Id1 promoter, which includes multiple Smad-binding elements, drives the expression of enhanced green fluorescent protein (eGFP), enabling live assessment of canonical Bmp/Smad1/5/8-mediated signaling (Figure IID in the online-only Data Supplement).[14] Confocal imaging of the emerging CVP revealed these mesenchymal shaped cells positioned at sites of anastomosis were Bmp-responsive (Figure IIE in the online-only Data Supplement). Higher resolution imaging of *Tg*(*BRE:eGFP)*; (*kdrl:mCherry)* embryos at ~26 hpf revealed that these BRE+ mesenchymal shaped cells made multiple contacts, through both their cell bodies and filopodial projections, with endothelial tip cell filopodia at putative sites of anastomosis (Figure 1A, middle and lower panels).Immunofluorescence staining with an antibody against phosphorylated-Smad1/5/8 (P-Smad1/5/8) revealed that these mesenchymal-shaped cells showed various degrees of nuclear P-Smad1/5/8 translocation, attesting to active Bmp signaling at least via ligands, Bmp2, 4 or 7 (Figure III in the online-only Data Supplement). Based on their morphology, we hypothesized that these BRE+ cells were mesenchymal stromal cells (SCs) previously shown to be crucial for the emergence of the caudal haemopoietic tissue (CHT) in zebrafish embryos[15,16] although their precise role in angiogenesis has hitherto remained unexplored.

To confirm the ontogeny of these cells, we performed time-lapse confocal microscopy on *Tg(BRE:eGFP)* embryos prior to onset of venous tip cell sprouting. At 20-22 hpf, several BRE+ cells detached from ventral ends of caudal somites through a process resembling epithelial-to-mesenchymal transition (EMT), acquiring a polarized morphology as they migrated ventrally towards the future site of CVP (Figure 1B, upper panel) (Figure IVA in the online-only Data Supplement). To confirm the identity of these cells as SCs, we used a Wnt signaling reporter *Tg(TCF:nls-mCherry),* which has been demonstrated to label nuclei of reticular SCs and their progenitors in zebrafish.[16] We crossed the *Tg(BRE:d2GFP)* fish, expressing destabilized GFP in Bmp-responsive cells, with the *Tg(TCF:nls-mCherry)* line to determine if these mesenchymal-shaped cells demonstrated active Bmp responses at sites of EMT. The destabilized GFP in the *Tg(BRE:d2GFP)* fish, due to its rapid turnover, provides a sensitive readout of dynamic Bmp responses in cells.[14] At 20 hpf, both *TCF:nls-mcherry*+ and *BRE:d2GFP*+ transgenes were co-expressed in the somites (Figure IVB–B’’’ in the online-only Data Supplement). Starting at approximately 22 hpf, the stromal progenitor cells budding out of ventral ends of caudal somites showed d2GFP+ cell bodies and mCherry+ nuclei (Figure 1B, lower panel) (Figure IVC–D’ in the online-only Data Supplement), confirming their identity as SCs.

Next, we sought to characterize the spatiotemporal patterns of SC-EC interactions to ascertain if SCs preferentially localized to sites of vessel fusion. At 24-25 hpf, prior to or coincident with tip cell induction, SCs exhibited a unique distribution pattern in which they lined up on the outside and at the ventral aspects of PCV, in close juxtaposition with ECs (Figure V in the online-only Data Supplement). We then employed time-lapse confocal microscopy to determine whether these SCs interacted with EC tip cells that sprout from the ventral ends of PCV at approximately the same time. Following tip cell induction,

SCs were positioned at the leading edge of endothelial tip cells, maintaining contacts with endothelial filopodia, and spearheading these tip cells as they migrated towards the avascular niche (64% of venous sprouts were spearheaded by SCs, N:8 embryos imaged) (Figure 1C) (Figure VI in the online-only Data Supplement).

At 26-28 hpf, at the ventromedial boundary, multiple putative sites of anastomosis had been established, of which approximately 90% were interposed by Bmp responsive SCs (N:21 embryos imaged). Based on this specific distribution pattern, we hypothesized that SCs actively partake in tip cell fusion in a manner analogous to macrophage chaperone cells described before.[2,8,17] Time-lapse confocal microscopy analyses revealed that SCs extended their protrusions to adjacent venous tip cells to create a connection that transiently spanned the distance between the two ipsilateral tip cells (Figure 1D). Next, we sought to determine if SCs overlay sites of tip cell fusion of the arterial-fated ISVs in the trunk, where these sprouts migrate in response to Vegfa gradients and fuse at the roof of the neural tube to create the dorsal longitudinal anastomotic vessel (DLAV).[12] However, our time-lapse confocal microscopy analysis revealed no Bmp-responsive SCs in or around sites of anastomosis during fusion of ipsilateral ISVs (Figure VII in the online-only Data Supplement). Further substantiating our observations, previous studies have revealed that anastomosis of dorsal aspects of ISVs is mediated by macrophage bridge cells during both developmental angiogenesis and following injury-induced revascularization of this region.[8,17,18] We also confirmed, using the *Tg(mpeg1:GFP);(kdrl:mCherry)* line, that mpeg1+ macrophages were frequently found at sites where ISVs inter-connect (Figure VIII in the online-only Data Supplement).

To test a functional role for SCs in mediating venous tip cell fusion, we selectively ablated them just prior to anastomosis. Specifically, we used a scanning confocal microscope, equipped with infrared (800 nm) laser, to identify a putative site of anastomosis (using 40X objective and digital zoom) and thereafter irradiated all SCs that were in close apposition to this site (ranging from 1 to 4 SCs per region of anastomosis), as per previously established protocol.[13] Time-lapse confocal analysis following ablation of SCs revealed that new SCs (emerging either from the ventral ends of caudal somites or from the adjacent milieu) started to re-colonize this region in minutes, an event which was subsequently ensued by tip cell fusion (Figure 1E) (Figure IX in the online-only Data Supplement)(Representative of 9 individual experiments). This dynamic and compensatory rearrangement of SCs and their recruitment to sites of anastomosis following ablation suggested that paracrine interactions between SCs and venous tip cells, at least in part, facilitate venous tip cell anastomosis.

To confirm that SC-EC interactions are crucial for anastomosis of venous tip cells at the angiogenic front of CVP, we used previously generated homozygous recessive maternal zygotic (MZ) syndecan 2 (*sdc2−/−*) mutants, in which a subset of SCs undergo apoptosis as they as bud out from ventral somites, resulting in significant attenuation of total SC counts in the embryo.[12] Although mutant embryos were overtly normal in appearance, when expressing the fluorescent endothelial reporter, *Tg(fli1:GFP)*, the *sdc2−/−* embryos displayed impaired and/or delayed angiogenesis as early as 25 hpf, evidenced by reduced numbers of venous sprouts emanating from ventral ends of PCV (Figure X in the online-only Data Supplement). When analyzed at 26-28 hpf, the developmental window during

which most anastomosis takes place, *sdc2−/−* embryos displayed an aberrant angiogenic pattern, evidenced by curtailed migratory behavior and smaller total CVP area than their wild-type siblings (Figure XI in the online-only Data Supplement). By 52 hpf, CVP development was significantly hampered in *sdc2−/−* embryos (Figure 1F, upper panel), demonstrated by reduced numbers of CVP loops and smaller mean CVP loop area (Figure 1F, lower panel). Taken together, these observations suggest a requirement for SCs in mediating the emergence and proper interaction of the first wave of angiogenic venous sprouts to establish a vascular plexi of adequate size in the developing embryo.

Next, because SCs showed high levels of Bmp responsiveness, we sought to determine if Bmp signaling was actively involved in the emergence of SCs and their interaction with endothelial tip cells. Beginning at ~22-24 hpf, *BRE:d2GFP* expression became progressively more prominent at the ventral ends of caudal somites and in the SC progenitors that emanated from this region, suggesting involvement of active Bmp signaling in mediating the development of SCs (Figure 2A–C) (Figure XII in the online-only Data Supplement). To determine the significance of Bmp signaling in SC emergence, we tested whether pharmacological inhibition of Bmp signaling would inhibit the emergence and ventral migration of SCs. Towards this goal, embryos were exposed to DMH1 (dorsomorphin homolog 1), a selective inhibitor of activin receptor-like kinase 2 (ALK2)(Selleckchem, Cat. No. S7146),[19] beginning at ~14-19 somites stages (~ 16 hpf), prior to onset of EMT from ventral somites. When imaged at 28-30 hpf, DMH1-treated embryos showed significantly reduced numbers of BRE+ SCs compared with those treated with DMSO, along with inhibition of venous angiogenesis, evidenced by significantly reduced numbers of endothelial sprouts, with no apparent curtailment of arterial-fated ISV sprouting (Figure 2D–G). Because DMH1 treatment inhibited both BRE+ SC numbers and venous sprouting, we tested whether the observed reduction in SC numbers was not secondary to inhibition of venous angiogenesis or due to absence of a vascular scaffold. To inhibit formation of a venous network independent of Bmp signaling, we used a previously established morpholino oligonucleotide (MO) to knockdown the expression of cardiac troponin T type 2a (*tnnt2a*). Loss of *tnnt2a* gives rise to a “silent heart phenotype” lacking cardiac contractions and blood flow, along with impaired venous angiogenesis and absence of a CVP.[20] Injection of ~2ng of *tnnt2a* MO resulted in complete inhibition of CVP formation as early as 28 hpf, with no apparent effects on ventral migration of SCs and their accumulation at the ventral aspects of PCV (FigureXIIIA and B in the online-only Data Supplement). By 52 hpf, despite failure of CVP development in *tnnt2a* morphants, no changes in the ventral migration or abundance of SCs were observed at the ventral ends of PCV (FigureXIIIC–E in the online-only Data Supplement). These results suggested that although both SCs and venous ECs maintain close spatiotemporal associations during development of CVP, the ventral migration of SCs is independent of a venous network. Further, these results suggest that Bmp signaling is required for the emergence of SCs from ventral somites and their interaction with ECs.

Overall, we show an endothelial cell-extrinsic mechanism facilitating venous tip cell fusion during developmental angiogenesis, mediated, at least in part, by Bmp-responsive and somite-derived SCs (FigureXIV in the online-only Data Supplement). The mechanisms by which SCs recognize and home into sites of anastomosis or how they facilitate bridging of tip cells remain unexplored. Do SCs facilitate venous angiogenesis through the release

of pro-angiogenic Bmps, with ECs expressing their cognate receptors, via direct cell-cell contact or in a paracrine fashion? Our observations suggest that SCs exhibit higher levels of Bmp responsiveness than adjacent tissues. This, coupled with the fact that pharmacological inhibition of Bmp signaling impairs SC-EC interactions, suggest that signaling via Bmp ligands, Bmp2, 4 or 7, at least in part, underlies the interphase of these inductive interactions between SCs and ECs. In addition to active involvement in anastomosis, our live imaging experiments suggest that SCs intimately interact with tip cells during the earliest stages of angiogenesis. This suggests that SCs facilitate tip cell induction and endothelial sprout elongation through cell-cell contacts.

The dorsally located somites, as paired blocks of mesoderm tissue distributed throughout the length of the embryo, serve to confine and guide arterial-fated ISVs by releasing pro-angiogenic Vegfs.[9] Here, our observations suggest that SCs originating from somites could act in a similar manner, but as mobile signaling nexuses or guiding posts, to control the timing, precision, and extent of Bmp-mediated venous invasion. SCs in the developed CVP were previously shown to interact with ECs to create an “endothelial pocket”, a transient niche that enables oriented division of hematopoietic stem cells.[15] Here, our observations reveal that these same SCs also serve a pro-angiogenic function, facilitating the development of CVP, which serves as the first hematopoietic stem cell niche in the embryo. In mammals, both mesoderm-derived SCs in the embryonic hematopoietic niche and neural crest-derived SCs in the fetal hematopoietic niches make intimate associations with ECs in the same milieu.[21,22] However, whether SCs play similar inductive roles in vascularization of embryonic or fetal hematopoietic niches in mammalian systems remains to be explored. Further, it remains unknown whether a pool of pro-angiogenic SCs is maintained and accessible throughout the lifetime of the organism and if they could also be instrumental in mediating angiogenesis in other contexts.

Supplementary Material

Refer to Web version on PubMed Central for supplementary material.

Acknowledgements:

The authors thank Dr. Sarah Childs (University of Calgary, Calgary) for kindly sharing their *Tg(6.5kdrl:mCherry)*^{ci5} zebrafish line. We thank Michael Cliff for their valuable help with zebrafish husbandry and for facilitating acquisition of all relevant zebrafish lines. The authors further thank Hannah Nonarath, Ayana Jamal and Tricia Slobodianuk for training and for their valuable discussions.

Sources of Funding:

Research was supported by a grant from the National Eye Institute, National Institutes of Health (R01EY29267) to Brian A. Link.

Nonstandard Abbreviations and Acronyms:

CVP	Caudal vein plexus
hpf	Hours post fertilization
DA	Dorsal artery

CHT	Caudal hematopoietic tissue
PCV	Posterior cardinal vein
SC	Stromal cell
ISV	Intersomitic vessel
MO	Morpholino oligonucleotide

References:

1-. Gerhardt H, Golding M, Fruttiger M, Ruhrberg C, Lundkvist A, Abramsson A, Jeltsch M, Mitchell C, Alitalo K, Shima D, Betsholtz C. VEGF guides angiogenic sprouting utilizing endothelial tip cell filopodia. J Cell Biol. 2003;161:1163–1177. doi: 10.1083/jcb.200302047. [PubMed: 12810700]

2-. Fantin A, Vieira JM, Gestri G, Denti L, Schwarz Q, Prykhozhij S, Peri F, Wilson SW, Ruhrberg C. Tissue macrophages act as cellular chaperones for vascular anastomosis downstream of VEGF-mediated endothelial tip cell induction. Blood. 2010; 116:829–840. doi: 10.1182/blood-2009-12-257832. [PubMed: 20404134]

3-. Rymo SF, Gerhardt H, Wolfhagen Sand F, Lang R, Uv A, Betsholtz C. A two-way communication between microglial cells and angiogenic sprouts regulates angiogenesis in aortic ring cultures. PLoS One. 2011 Jan 10;61:e15846. doi: 10.1371/journal.pone.0015846.

4-. Okabe K, Kobayashi S, Yamada T, Kurihara T, Tai-Nagara I, Miyamoto T, Mukouyama YS, Sato TN, Suda T, Ema M, Kubota Y. Neurons limit angiogenesis by titrating VEGF in retina. Cell. 2014; 159:584–596. doi: 10.1016/j.cell.2014.09.025. [PubMed: 25417109]

5-. Ando K, Fukuhara S, Izumi N, Nakajima H, Fukui H, Kelsh RN, Mochizuki N. Clarification of mural cell coverage of vascular endothelial cells by live imaging of zebrafish. Development. 2016;143:1328–1339. doi: 10.1242/dev.132654. [PubMed: 26952986]

6-. Matsuoka RL, Marass M, Avdesh A, Helker CS, Maischein HM, Grosse AS, Kaur H, Lawson ND, Herzog W, Stainier DY. Radial glia regulate vascular patterning around the developing spinal cord. Elife. 2016;5:e20253. doi: 10.7554/eLife.20253. [PubMed: 27852438]

7-. Nesmith JE, Chappell JC, Cluceru JG, Bautch VL. Blood vessel anastomosis is spatially regulated by Flt1 during angiogenesis. Development. 2017;144:889–896. doi: 10.1242/dev.145672. [PubMed: 28246215]

8-. Fantin A, Vieira JM, Plein A, Denti L, Fruttiger M, Pollard JW, Ruhrberg C. NRP1 acts cell autonomously in endothelium to promote tip cell function during sprouting angiogenesis. Blood. 2013;121:2352–2362. doi: 10.1182/blood-2012-05-424713. [PubMed: 23315162]

9-. Kim JD, Lee HW, Jin SW. Diversity is in my veins: role of bone morphogenetic protein signaling during venous morphogenesis in zebrafish illustrates the heterogeneity within endothelial cells. Arterioscler Thromb Vasc Biol. 2014;34:1838–1845. doi: 10.1161/ATVBAHA.114.303219. [PubMed: 25060789]

10-. Neal A, Nornes S, Payne S, Wallace MD, Fritzsche M, Louphrasitthiphol P, Wilkinson RN, Chouliaras KM, Liu K, Plant K, Sholapurkar R, Ratnayaka I, Herzog W, Bond G, Chico T, Bou-Gharios G, De Val S. Venous identity requires BMP signalling through ALK3. Nat Commun. 2019;10:453. doi: 10.1038/s41467-019-08315-w. [PubMed: 30692543]

11-. Pibouin-Fragner L, Eichmann A, Pardanaud L. Environmental and intrinsic modulations of venous differentiation. Cell Mol Life Sci. 2022;79:491. doi: 10.1007/s00018-022-04470-4. [PubMed: 35987946]

12-. Lamichhane BS, Bisgrove BW, Su Y, Demarest BL, Yost HJ. Syndecan 2 regulates hematopoietic lineages and infection resolution in zebrafish. bioRxiv 2020.05.04.076786. doi: 10.1101/2020.05.04.076786.

13-. Volpe BA, Fotino TH, Steiner AB. Confocal Microscope-Based Laser Ablation and Regeneration Assay in Zebrafish Interneuromast Cells. J Vis Exp. 2020;(159):10.3791/60966. doi: 10.3791/60966.

14-. Collery RF, Link BA. Dynamic smad-mediated BMP signaling revealed through transgenic zebrafish. Dev Dyn. 2011;240:712–722. doi: 10.1002/dvdy.22567. [PubMed: 21337469]

15-. Tamplin OJ, Durand EM, Carr LA, Childs SJ, Hagedorn EJ, Li P, Yzaguirre AD, Speck NA, Zon LI. Hematopoietic stem cell arrival triggers dynamic remodeling of the perivascular niche. Cell. 2015;160:241–252. doi: 10.1016/j.cell.2014.12.032. [PubMed: 25594182]

16-. Murayama E, Sarris M, Redd M, Le Guyader D, Vivier C, Horsley W, Trede N, Herbomel P. NACA deficiency reveals the crucial role of somite-derived stromal cells in haematopoietic niche formation. Nat Commun. 2015;6:8375. doi: 10.1038/ncomms9375. [PubMed: 26411530]

17-. Gurevich DB, Severn CE, Twomey C, Greenhough A, Cash J, Toye AM, Mellor H, Martin P. Live imaging of wound angiogenesis reveals macrophage orchestrated vessel sprouting and regression. EMBO J. 2018;37:e97786. doi: 10.15252/embj.201797786. [PubMed: 29866703]

18-. Gerri C, Marín-Juez R, Marass M, Marks A, Maischein HM, Stainier DYR. Hif-1α regulates macrophage-endothelial interactions during blood vessel development in zebrafish. Nat Commun. 2017;8:15492. doi: 10.1038/ncomms15492. [PubMed: 28524872]

19-. Hao J, Ho JN, Lewis JA, Karim KA, Daniels RN, Gentry PR, Hopkins CR, Lindsley CW, Hong CC. In vivo structure-activity relationship study of dorsomorphin analogues identifies selective VEGF and BMP inhibitors. ACS Chem Biol. 2010;5:245–253. doi: 10.1021/cb9002865. [PubMed: 20020776]

20-. Kugler E, Snodgrass R, Bowley G, Plant K, Serbanovic-Canic J, Hamilton N, Evans PC, Chico T, Armitage P. The effect of absent blood flow on the zebrafish cerebral and trunk vasculature. Vasc Biol. 2021;3:1–16. doi: 10.1530/VB-21-0009. [PubMed: 34522840]

21-. Chandrakanthan V, Rorimpandey P, Zanini F, Chacon D, Olivier J, Joshi S, Kang YC, Knezevic K, Huang Y, Qiao Q, Oliver RA, Unnikrishnan A, Carter DR, Lee B, Brownlee C, Power C, Brink R, Mendez-Ferrer S, Enikolopov G, Walsh W, Göttgens B, Taoudi S, Beck D, Pimanda JE. Mesoderm-derived PDGFRA+ cells regulate the emergence of hematopoietic stem cells in the dorsal aorta. Nat Cell Biol. 2022;24:1211–1225. doi: 10.1038/s41556-022-00955-3. [PubMed: 35902769]

22-. Khan JA, Mendelson A, Kunisaki Y, Birbrair A, Kou Y, Arnal-Estapé A, Pinho S, Ciero P, Nakahara F, Ma'ayan A, Bergman A, Merad M, Frenette PS. Fetal liver hematopoietic stem cell niches associate with portal vessels. Science. 2016;351:176–180. doi: 10.1126/science.aad0084. [PubMed: 26634440]

Highlights:

- Mesoderm-derived mesenchymal stromal cells (SCs) are highly responsive to BMPs.
- SCs facilitate venous tip cell induction and anastomosis downstream of BMP signaling.
- Loss of SCs impairs venous plexus formation.

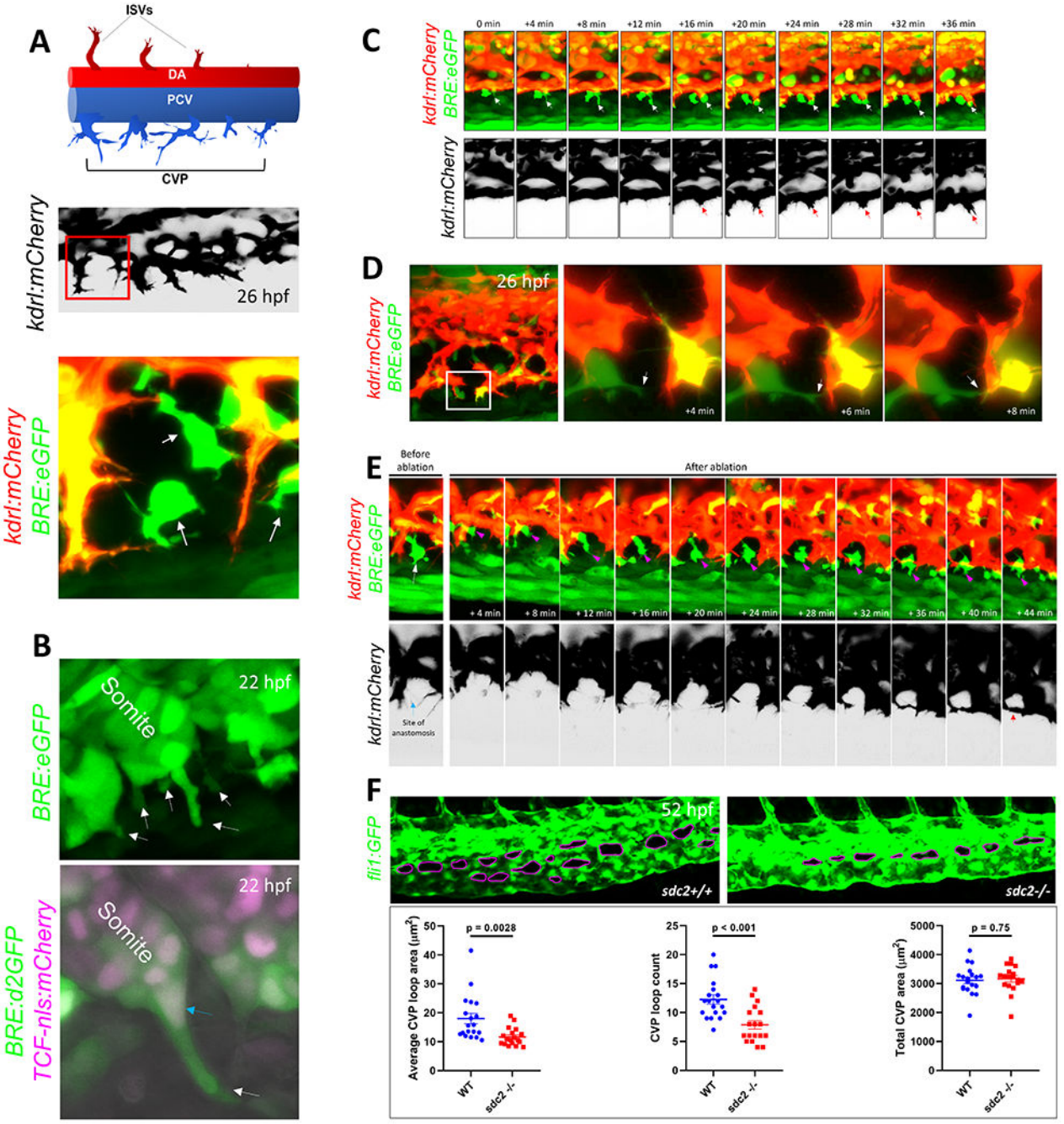

Figure 1. Mesenchymal stromal cells facilitate venous tip cell fusion during BMP-dependent venous angiogenesis.

(**A**) Axial vessels in embryonic zebrafish and the angiogenic sprouts that emanate from them. **Top**, Schematic depiction of the dorsal artery (DA) and DA-derived intersomitic vessels (ISVs), along with the posterior cardinal vein (PCV) and venous sprouts that make up the caudal vein plexus (CVP). **Middle**, Maximum projection confocal micrograph of a 26-hour post fertilization (hpf) embryo, showing venous sprouts emerging from the ventral ends of PCV, as revealed by *kdrl:mCherry* expression. Inverted black/white image. Multiple

endothelial sprouts are shown. **Lower**, Higher magnification of the red boxed region in the middle panel, showing a putative site of anastomosis and multiple filopodial protrusions emerging from endothelial sprouts. Several BMP-responsive (BRE+) mesenchymal-shaped cells are found interposing sites of anastomosis in a *Tg(BRE:eGFP);(kdrl:mCherry)* double transgenic embryo. (**B**) Mesenchymal stromal cells (SCs) interpose sites of anastomosis. **Top**, Still image from a time-lapse maximum projection confocal micrograph of a 22 hpf *Tg(BRE:eGFP)* embryo, showing a number BRE+ cells emerging from ventral somites. White arrows point to BRE+ cells budding out of ventral somites. **Bottom**, Maximum projection confocal micrograph of a 22 hpf *Tg(BRE:d2GFP);(TCF-nls:mCherry)* embryo. High resolution imaging revealed that SC progenitors express d2GFP in the cytoplasm and mCherry in the nuclei. (**C**) Stills from time-lapse confocal microscopy of ventral PCV at 24 hpf in a *Tg(BRE:eGFP);(kdrl:mCherry)* embryo, showing the spatio-temporal association of a SCs with an endothelial tip cell during tip cell induction and sprouting. Maximum projection images are shown. White arrow points to SC; red arrow the sprouting tip cell. (**D**) SCs facilitate anastomosis through cell-cell interaction. **Left**, Maximum projection confocal image of part of the CVP region at 26 hpf in a Tg(*BRE:eGFP);(kdrl:mCherry)* embryo, showing several putative sites of anastomosis. **Right**, Stills from time-lapse confocal microscopy of the white boxed region at higher magnification. The white arrow points to SC filopodial protrusion extending to the adjacent tip cell. Brightness and contrast for the entire image were adjusted using the ImageJ/Fiji software (National Institutes of Health) to reveal filopodial structures. (**E**) Laser ablation of SCs at sites of anastomosis is ensued by recruitment of new SCs, followed by anastomosis. Stills from time-lapse confocal microscopy analysis of *Tg(BRE:eGFP);(kdrl:mCherry)* embryo, showing a putative site of anastomosis (blue arrow) prior to laser ablation and a BRE+ SC (white arrow) in the same vicinity. Following irradiation of this SC with 800 nm laser, a new SC gravitates to the same site of anastomosis within minutes, concomitant with completion of anastomosis. The magenta arrow points to the newly emerging SC. Red arrow indicates that a CVP loop is established following anastomosis. (**F**) Partial loss of SCs in sdc2−/− embryos results in impaired venous angiogenesis. **Top**, Representative maximum projection confocal micrographs of part of the CVP region in wild-type and homozygous recessive maternal zygotic (MZ) syndecan 2 (*sdc2−/−*) mutants, expressing the endothelial-specific *Tg(fli1:GFP)* transgene. The caudal vein plexus loops (CVP loops) in wild-type and *sdc2−/−* mutants are outlined in magenta. All images are lateral, with anterior to the left. **Bottom**, Quantification of average CVP loop area, CVP counts and total CVP area at 52 hpf are shown. P-values are shown. An unpaired student's t-test was used to compare between wild-type fish (N:19 embryos) and *sdc2*−/− siblings (N:18 embryos).

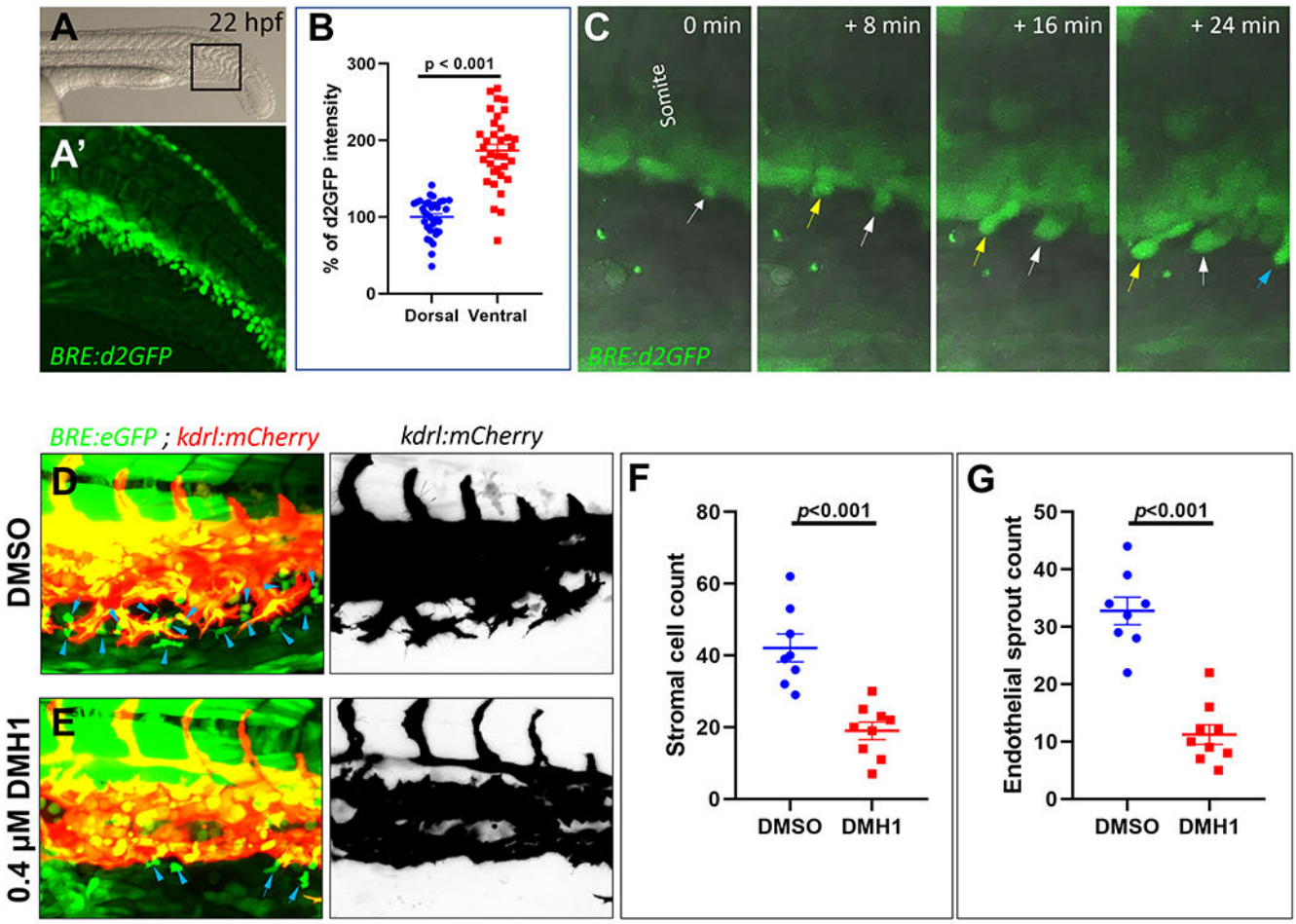

Figure 2. Bone morphogenic protein (Bmp) signaling is required for the emergence of pro-angiogenic mesenchymal stromal cells (SCs).

(A) Representative brightfield photomicrograph of the trunk and tail region of a ~22-hour post fertilization (hpf) *Tg(BRE:d2GFP)* embryo. Lateral image, with anterior to left. **(A')** Maximum projection confocal micrograph of the black-boxed region in A. **(B)** Quantification of destabilized green fluorescent protein (d2GFP) intensity in dorsal and ventral aspects of somites in ~22 hpf *Tg(BRE:d2GFP)* embryos (N:34 embryos of comparable developmental stages were imaged). **(C)** Maximum intensity projection still images from time-lapse confocal imaging of part of the caudal somites in a *Tg(BRE:d2GFP)* embryo, combined with differential phase contrast imaging in grey, showing emergence of BRE+ SCs from ventral aspects of caudal somites. Different colored arrows point to distinct SC populations emerging from ventral somites over time **(D and E)** Maximum projection confocal microscopy analysis of the emerging caudal vein plexus (CVP) in ~28 hpf *Tg(BRE:eGFP);(kdrl:mCherry)* embryos treated either with DMSO or DMH1 (400 nM), beginning at ~14-19 somites stages (~ 16 hpf). **(F)** Quantification of SC counts in the CVP region of DMSO-treated embryos (N:8 embryos) versus DMH1 (400 nM)-treated embryos

(N:9 embryos). **(G)** Quantification of endothelial sprout numbers in the same DMSO-treated versus DMH1 (400 nM)-treated embryos.